

Dynamic Model for Real-Time Estimation of Aerodynamic Characteristics

Jiang Quanwei* and Chen Qiongang†

China Aerodynamic Research and Development Center, Sichuan, China

A six-degree-of-freedom dynamic model is presented in this paper. Using the model and an extended Kalman filter algorithm (EKF), the problem of the real-time identification of the aerodynamic characteristics of a re-entry body is investigated and a large number of numerical simulations are conducted. A detailed comparison is made between the present model and an ordinary model. The present model obviates the somewhat impractical assumptions about altitude measurements and atmospheric modeling made in the ordinary model, and is capable of estimating aerodynamic coefficient ratios, including the important static stability margin. Furthermore, the convergence time and model errors of the two models are analyzed and compared. The results show that the present model has greater applicability as compared with the ordinary model.

Nomenclature

C_x	= axial force coefficient
$C_{N\alpha}$	= normal force derivative
$C_{m\alpha}$	= static moment derivative
C_l	= roll moment coefficient
C_{mq}	= damping derivative
d	= base diameter
g	= gravity acceleration
I_x, I	= moments of inertia
m	= mass
P_k	= state covariance matrix
p, q, r	= angular rates
\bar{q}	= dynamic pressure
S	= base area
T_c	= computer time required for convergence estimation
T_f	= flight time required for convergence estimation
t	= time
u, v, w	= velocity components
V	= total velocity
α, β	= angles of attack and sideslip
θ, ϕ	= Euler angles
ρ	= atmospheric density

Superscripts

$(\hat{})$	= optimal estimate
$[\]^T$	= transpose

Subscript

k	= measurement order number
-----	----------------------------

Introduction

IN order to effectively and accurately control modern high-performance vehicles such as missiles, airplanes, and re-entry bodies, the aerodynamic characteristics of the vehicle must be estimated perfectly. For many reasons, the predicted aerodynamic performance using ground wind-tunnel tests or aero-

dynamic calculations is often different from that in real flight. Another approach in resolving this problem is to use onboard measurements and a computer to make a real-time estimation of the aerodynamic characteristics in flight, which is then used to draw up the control signals to arrive at an accurate control. With the rapid development of modern aircraft and electronic technology, the need for real-time estimation is getting more and more urgent and realistic. In terms of real-time estimation of aerodynamic coefficients from high-speed vehicles such as the re-entry bodies, the main difficulties are as follows: 1) it is required that both onboard computer and its software have the real-time processing capability with high accuracy and limited storages; 2) it is difficult to measure the flight altitudes using a radar on the vehicle due to the effect of the plasma; and 3) because the range of flight altitudes is great, a simple atmospheric model adopted sometimes cannot represent the real cases.^{1,2}

In the case of re-entry flight, Kelsey^{3,4} made a preliminary study of the real-time identification of the aerodynamic characteristics. His emphasis was placed on part of the first difficulty just mentioned, trying to find a proper dynamic model that could identify properly the major aerodynamic characteristics such as the static moment derivative as well as to meet the requirements for real-time processing. He came to the conclusion that a near-real-time estimation was possible if the accuracy and speed of the onboard computer were similar to that of CDC 6600. His work, however, evaded the other two difficulties, making two assumptions: 1) the altitudes were accurately measured by an onboard radar altimeter, and 2) the relationship between atmospheric density and altitude was modeled as a simple exponential function.

The purpose of the paper is to attempt to estimate the major aerodynamic characteristics in the absence of Kelsey's two assumptions and without increasing estimation time. The technical approach is to transform the six-degree-of-freedom dynamic model to become independent of flight altitudes and atmospheric density by using the relations of the measured accelerations and such quantities as dynamic pressure, normal force derivative, and angles of attack. Then, by means of the extended Kalman filter algorithm, a set of aerodynamic coefficient ratios is identified, including the important static stability margin.

It is well known that lift-to-drag ratio and aerodynamic center of pressure are independent of flight dynamic pressure. The features of the present model, however, are such that the model is based upon six-degree-of-freedom dynamic equations containing general derivative ratios or coefficient ratios.

Presented as Paper 86-2224 at the AIAA/AAS Atmospheric Flight Mechanics Conference, Williamsburg, VA, Aug. 18-20, 1986; received Jan. 11, 1987; revision received May 3, 1988. Copyright © American Institute of Aeronautics and Astronautics, Inc., 1986. All rights reserved.

*Associate Research Professor.

†Engineer.

The present paper continues and extends the author's previous work,^{5,6} which focuses on posttest identification where the dynamic model is implicit; this paper falls into real-time identification where the model is explicit. First the work by Kelsey is reviewed. This is followed by a derivation of the present model. The numerical simulation results are then discussed and compared with Kelsey's. Finally, several conclusions are given.

Model Based on Altitude Measurements

Kelsey investigated 10 cases of a six-degree-of-freedom dynamic model to examine the effects of varied state-measurement-parameter combinations on identification accuracy and real-time calculating capability. The state variables were chosen to be measurements, namely the body-referenced inertial velocities u, v, w and the body-referenced angular rates p, q, r , which were measured by onboard integrating accelerometers and rate gyros, respectively. The gravitational force was ignored in the model. The details can be found in Ref. 3. For detailed comparison here, only Kelsey's case 5 is elaborated upon as an example. For simplicity, Kelsey's model will be referred to as the "K-model." The vector of dynamic states Y , the vector of parameters C , and the vector of measurements h are given as

$$\begin{aligned} Y &= [u \ v \ w \ p \ q \ r]^T \\ C &= [C_l \ C_{m\alpha}]^T \\ h &= [u \ v \ w \ p \ q \ r]^T \end{aligned} \quad (1)$$

For linear and symmetric aerodynamic characteristics, the dynamic model based on body-referenced six-degree-of-freedom motion equations is given:

$$\dot{u} = C_x \bar{q} S / m - wq + vr$$

$$\dot{v} = C_{N\alpha} \beta \bar{q} S / m - ur + pw$$

(In literature this equation is often expressed as $\dot{v} = -C_{N\alpha} \beta \bar{q} S / m - ur + pw$.)

$$\dot{w} = -C_{N\alpha} \alpha \bar{q} S / m - vp + qu$$

$$\dot{p} = C \bar{q} S d / I_x$$

$$\dot{q} = (\bar{q} S d / I) [C_{m\alpha} \alpha + C_{mq} q (d/2V)] + pr(1 - I_x/I)$$

$$\dot{r} = (\bar{q} S d / I) [-C_{m\alpha} \beta + C_{mq} r (d/2V)] - pq(1 - I_x/I) \quad (2)$$

where

$$V = (u^2 + v^2 + w^2)^{1/2} \quad (3)$$

$$\alpha = \tan^{-1}(w/u) \quad (4)$$

$$\beta = \tan^{-1}(v/u) \quad (5)$$

[This equation may be taken as $\beta = \sin^{-1}(v/V)$.]

$$\bar{q} = 0.5 \rho V^2 \quad (6)$$

It was assumed that flight altitudes z could be measured by an onboard radar and that ρ was a simple exponential function of the altitudes

$$\rho = 0.00237692(1.0 + 6.875 \times 10^{-6} z)^{4.2561} \quad (7)$$

Coefficients C_x , $C_{N\alpha}$, and C_{mq} , which were not augmented into the vector of parameters, and such quantities as S , m , d , I , and I_x , were all known constants. The preceding equations constituted Kelsey's identification model.

The outline of the numerical simulation process is as follows. First the simulated measurement data, u, v, w, p, q, r , and flight altitudes z were generated based on the complete dynamic differential equations, including gravity and relevant conditions. These data were then stored in the machine in discrete form. The recursive calculations proceeded using the mentioned model combined with EKF formulas in order to estimate the aerodynamic coefficients optimally.

The so-called "gain-innovations product" ϵ_k was used as a convergence index:

$$\epsilon_k = K_k v_k \quad (8)$$

$$v_k = Z_k - h_k[\hat{X}_k(-)] \quad (9)$$

where K_k is the Kalman gain matrix, Z_k the measurement data vector, and $\hat{X}_k(-)$ the predicted state estimate. The convergence was considered achieved when a certain average of ϵ_k fell below a preset value.

Present Model

Only a common assumption is made that the onboard accelerometers could provide the lateral accelerations a_y and a_z at the center of gravity. The equations that relate such quantities as a_y , a_z , \bar{q} , $C_{N\alpha}$, α , and β are

$$\begin{aligned} a_y &= \bar{q} S C_{N\alpha} \beta / m \\ a_z &= \bar{q} S C_{N\alpha} \alpha / m \end{aligned} \quad (10)$$

Combining these equations yields

$$\bar{q} S = (m / C_{N\alpha}) (A / \eta) \quad (11)$$

where

$$A = (a_y^2 + a_z^2)^{1/2} \quad (12)$$

is the resultant lateral acceleration and

$$\eta = (\alpha^2 + \beta^2)^{1/2} \quad (13)$$

is the resultant angle of attack. Substituting Eq. (11) into Eq. (2) and defining "the coefficient ratios"

$$\begin{aligned} \bar{C}_x &= C_x / C_{N\alpha}, & \bar{C}_1 &= C_1 / C_{N\alpha} \\ \bar{C}_{m\alpha} &= C_{m\alpha} / C_{N\alpha}, & \bar{C}_{mq} &= C_{mq} / C_{N\alpha} \end{aligned} \quad (14)$$

results in

$$\dot{u} = \bar{C}_x A / \eta - wq + vr$$

$$\dot{v} = \beta A / \eta - ur + pw$$

$$\dot{w} = -\alpha A / \eta - vp + qu$$

$$\dot{p} = \bar{C}_1 (md / I_x) (A / \eta)$$

$$\dot{q} = (md / I) (A / \eta) [\bar{C}_{m\alpha} \alpha + \bar{C}_{mq} q (d/2V)] + pr(1 - I_x/I)$$

$$\dot{r} = (md / I) (A / \eta) [-\bar{C}_{m\alpha} \beta + \bar{C}_{mq} r (d/2V)] - pq(1 - I_x/I) \quad (15)$$

where

$$V = (u^2 + v^2 + w^2)^{1/2} \quad (16)$$

If it is assumed that the angle of attack and angle of sideslip are small, Eqs. (4) and (5) may be simplified as

$$\alpha = w/u \quad (17)$$

$$\beta = v/u \quad (18)$$

and so

$$\eta = (v^2 + w^2)^{1/2}/u \quad (19)$$

Thus, Eqs. (14–19) constitute the present identification model. Here, Y , C , and h are

$$\begin{aligned} Y &= [u \ v \ w \ p \ q \ r]^T \\ C &= [\bar{C}_x \ \bar{C}_l \ \bar{C}_{m\dot{x}} \ \bar{C}_{m\dot{q}}]^T \\ h &= [u \ v \ w \ p \ q \ r]^T \end{aligned} \quad (20)$$

and the values of A are also measured and given in the form of discrete sampling.

Compared with the K-model, the present model has two features: 1) it is independent of altitude measurements and atmospheric model; and 2) the aerodynamic parameters appear in the form of coefficient ratios. The present model is referred to as "the model of no outside measurements."

) In order to correspond to case 5 of the K-model, this paper analyzes only

$$C = [\bar{C}_l \ \bar{C}_{m\dot{x}}]^T \quad (21)$$

The $\bar{C}_{m\dot{x}}$ is an important parameter that represents the static stability of an aircraft, referred to as the static stability margin. Parameters \bar{C}_x and $\bar{C}_{m\dot{q}}$, which are not augmented into the vector of parameters, and such quantities as m , d , I , and I_x , are known constants.

Note the major differences between the present model and the model of Ref. 6: 1) the aerodynamic coefficient ratios \bar{C} appear explicitly in the present model and implicitly in Ref. 6; 2) Ref. 6 contains explicitly the atmospheric model and altitudes, which the present model has nothing to do with; and 3) the present paper requires measurements u , v , and w , but Ref. 6 does not make these measurements.

Table 1 Initial conditions

Initial conditions for generating measurements			
Physical constants	Aerodynamic coefficients	Initial states	
$d = 1.25 \text{ ft}$	$C_x = -0.06$	$u = 12,000 \text{ ft/s}$	$\theta = -0.5 \text{ rad}$
$S = 1.227 \text{ ft}^2$	$C_{m\dot{q}} = -20.0 \text{ rad}^{-1}$	$v = 0.0$	$\phi = 0.0$
$I_x = 1.5 \text{ slug-ft}^2$	$C_{m\dot{x}} = -0.7 \text{ rad}^{-1}$	$w = 209.46 \text{ ft/s}$	$z = -100,000.0 \text{ ft}$
$I = 20.0 \text{ slug-ft}^2$	$C_{N\dot{x}} = 4.0 \text{ rad}^{-1}$	$p = 10.0 \text{ rad/s}$	
$m = 8.0 \text{ slug}$	$C_l = 0.0$	$q = 0.0$	
$g = 32.174 \text{ ft/s}^2$		$r = 0.0$	
Nominal standard deviations			
Measurements	Initial states	Initial aerodynamic coefficient	
$u, v, w = 3.16 \text{ ft/s}$	$u = 14.14 \text{ ft/s}$	$C_l = 0.1$	
$p, q, r = 0.1 \text{ rad/s}$	$v, w = 10.0 \text{ ft/s}$	$C_{m\dot{x}} = 0.265 \text{ rad}^{-1}$	
	$p, q, r = 0.707 \text{ rad/s}$		

Table 2 Filtering results of two models

Filtering results							
Number of groups	Calculating case	T_f (k)		T_c (T_c/T_f)		$\bar{C}_{m\dot{x}}$ ($\bar{C}_{m\dot{x}}/\bar{C}_{m\dot{q}}$)	
		K-model	Present model	K-model	Present model	K-model	Present model
1	$Dt = 0.02$	0.66 (33)	0.68 (34)	54.5 (82.6)	53.4 (78.5)	-0.698 (0.997)	-0.699 (0.999)
2	$Dt = 0.01$	0.52 (52)	0.52 (52)	42.9 (82.5)	40.8 (78.5)	-0.699 (0.999)	-0.694 (0.991)
3	$Dt = 0.03$	0.69–0.99 ^a (23–33)	0.81 (27)	56.9–81.7 (82.5)	63.6 (78.5)	-0.700 (1.000)	-0.702 (1.003)
4	$0.5R_k$	0.64 (32)	0.68 (34)	52.8 (82.5)	53.4 (78.5)	-0.699 (0.999)	-0.700 (1.000)
5	$2.0R_k$	0.68–0.88 (34–44)	0.70 (35)	56.1–72.6 (82.5)	55.0 (78.6)	-0.697 (0.996)	-0.698 (0.997)
6	$0.5P_0$	0.66 (33)	0.68 (34)	54.5 (82.5)	53.4 (78.5)	-0.698 (0.997)	-0.699 (0.999)
7	$2.0P_0$	0.66 (33)	0.68 (34)	54.5 (82.5)	53.4 (78.5)	-0.698 (0.997)	-0.699 (0.999)

^aTwo values are due to the variations of the convergence index ϵ_k .

Numerical Results and Discussion

For comparison, the initial conditions and their units used in the simulation were chosen to be the same as those in Ref. 3 (see Table 1). The simulated measurement data $u, v, w, p, q,$ and r generated by the computer are shown in Figs. 1 and 2. The initial parameters correspond to a flight velocity of 12,000 ft/s, and altitude of 100,000 ft, a re-entry angle of -28.7° , maximum angle of attack of 1° , and a roll rate of 10 rad/s. A flight trajectory section of about $2''$ was simulated, and only of $0.8''$ is shown in the figures. The measurement noise was added on all the data. Figure 2 shows that the measurement noise level added on the angular rates q and r is so large that the resulting data points hardly reflect the variation of the ideal states. (The dotted lines in the figures are the noise-free theoretical curves.) Figure 3 shows the onboard noise-free observation of the resultant lateral accelerations A and flight altitudes z used in the filtering of the present model and K-model, respectively.

The identification calculations of both the K-model and the present model were based on the same simulated measurement data. The EKF formulas, the calculation procedure, the initial data, and the convergence index were the same for both models.

The filtering results of the two models are shown in Table 2. Seven different cases were simulated, the first group being the typical case. The sampling interval Δt was taken as 0.02 s. The second and third groups investigated the effects of Δt . The fourth and fifth groups investigated the effects of measurement noise R_k ; e.g. the value of R_k in the fourth group was half the value of R_k in the first group, and the value of R_k in the fifth group was double the value of R_k in the first group. The sixth and seventh groups investigated the effects of the initial variances P_0 .

The filtering results of the first group in Table 2 indicate that, with the same convergence index, the difference of T_f required for filtering in both models is very small. The values of T_f are 0.66 s for the K-model and 0.68 s for the present model, corresponding to the measurement order numbers of $k = 33$ and $k = 34$, respectively. At the same time, T_c in a 320-type computer is 54.5 s for the K-model and 53.4 s for the present model; i.e., the latter is faster by 1.1 s. As for estimate accuracies of C_{mx} , the values of \hat{C}_{mx} are -0.699 for the present model and -0.698 for the K-model. They are quite consistent with the true value of -0.7 . For C_b , both models yielded correct estimates with an absolute error of about 5×10^{-5} .

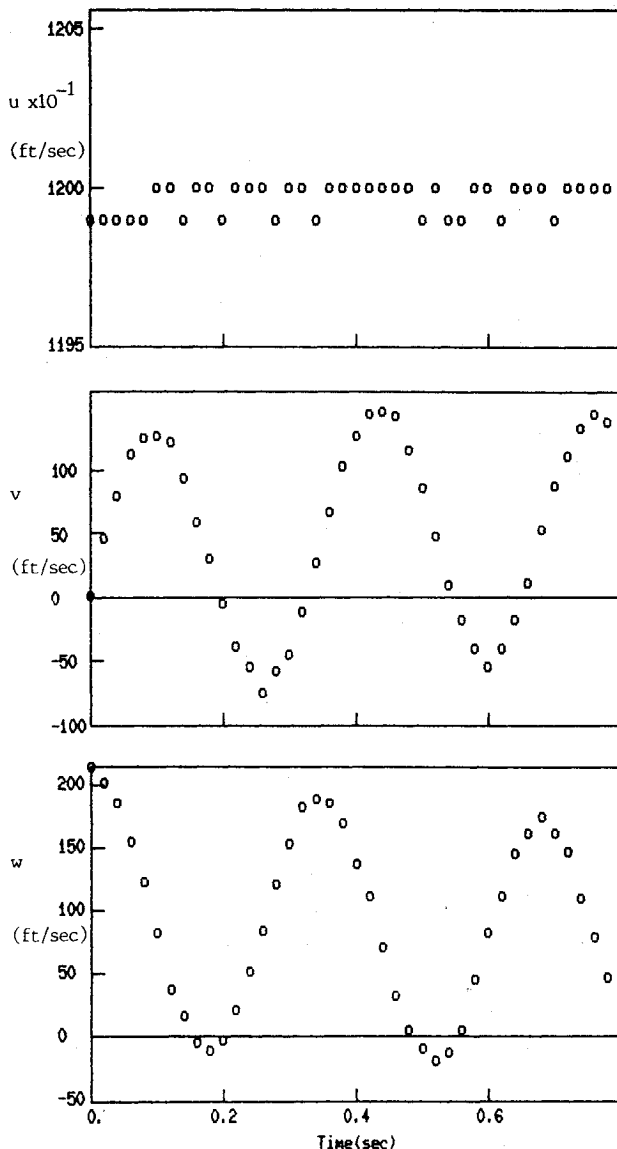


Fig. 1 Simulated measurements u, v, w .

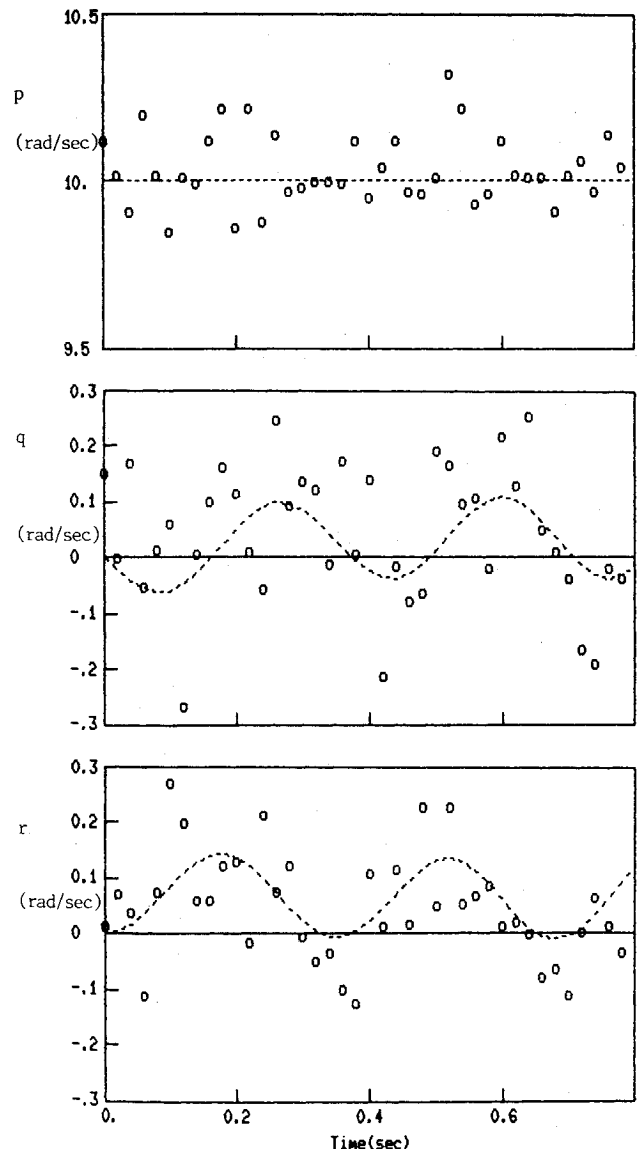
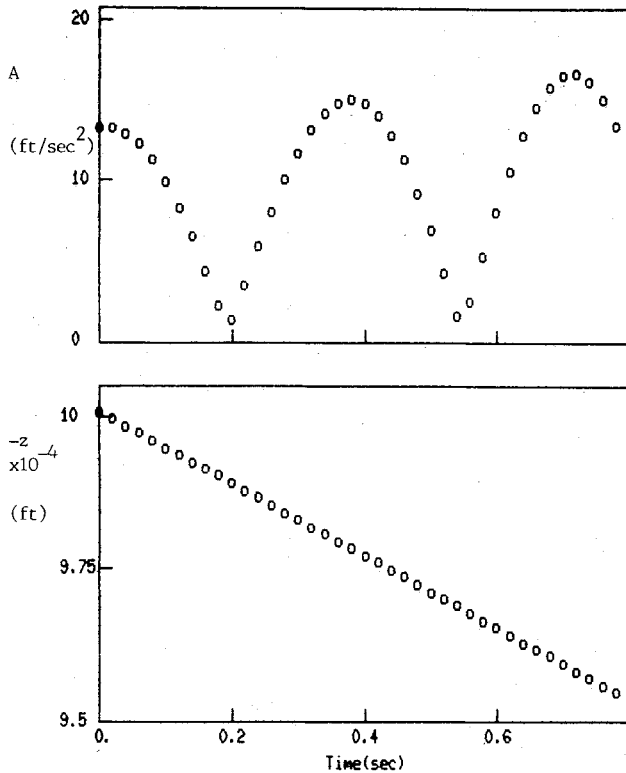


Fig. 2 Simulated measurements p, q, r .

Fig. 3 Simulated measurements A , z .

Comparing the results of the first group with those of the others, it is derived that 1) the values of T_f and T_c are decreased by reducing the sampling intervals, 2) the estimation accuracies are slightly degraded by increasing the measurement noise, 3) the variation of the state initial variances has little effect on the filtering results, 4) the value of T_f is about 0.7 s, 5) the values of T_c/T_f are 78.5 for the present model and 82.5 for the K-model, and 6) the relative errors of the static moment derivative are mostly less than 0.3%, with a maximum value of no more 1%. The filtering histories of a typical case are shown in Figs. 4–6.

The filtering history of the static stability derivative $\hat{C}_{m\alpha}$ is shown in Fig. 4, in which the solid lines and the dotted lines correspond to the present model and the K-model, respectively. Expression $\hat{C}_{m\alpha}$ and $\varepsilon_k(t)$, $P_k(t)$ are plotted in three subfigures. These figures demonstrate similar convergence processes for both models. Although the initial estimate errors were very large, the errors decreased to less than 10% just after 0.2-s filtering, and when the filtering went on for 0.4 s, the errors had decreased to nearly 1%. It was interesting that after $t = 0.4$ s, the histories of the $\hat{C}_{m\alpha}(t)$ and $\varepsilon_k(t)$ of both models began to overlap. This indicates that the filtering results were not sensitive to the model errors, including mainly neglecting gravity force, approximations of small angles of attack, and interpolations of the resultant lateral accelerations A . When the initial angle of attack increased to 10 deg, the mentioned characteristics remained unchanged. Figure 4c shows that the plots of the $P_k(t)$ of both models are very close.

The filtering histories of \hat{C}_l are shown in Fig. 5. Though the initial errors are very large, the curves converge very rapidly. For clarity, only the case of $t \leq 0.24$ s is shown in the figure, and after $t = 0.06$ s, the curves have been amplified to demonstrate variations of small quantities. As shown in this figure, both models exhibit favorable convergence characteristics.

Four filtering histories of $\hat{C}_{m\alpha}$ of the present model are shown in Fig. 6, each corresponding to one set of initial states generated randomly. The figure shows that all curves converge to the true value in the same manner, though their initial

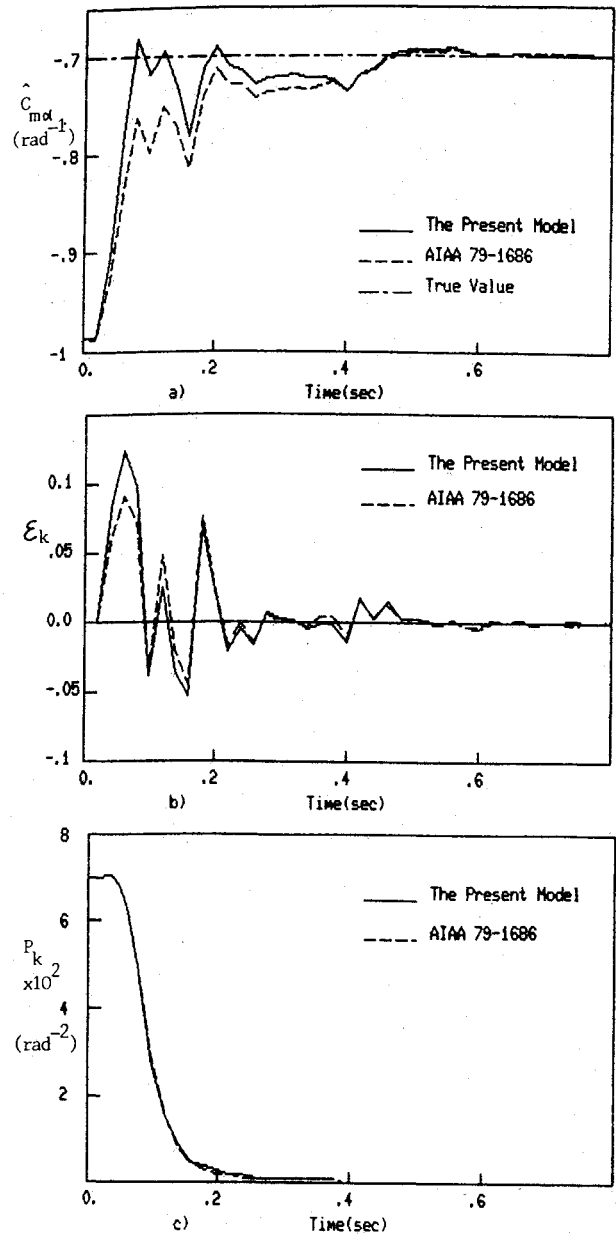


Fig. 4 Static moment derivative: a) estimate; b) gain innovations product; c) variance.

values are significantly different. In the same figure, the point lines denote the computed standard deviations by the filter, $\sqrt{(P_k)}$, and four sets of the point lines appear the same. This figure also shows clearly that the curves of $\hat{C}_{m\alpha}$ are quite consistent with the point lines in the statistical sense. In other words, the present model and the K-model possess equivalent real-time estimation capability and accuracy. It is important to note that coefficient ratios $\bar{C}_{m\alpha} = \hat{C}_{m\alpha}/C_{N\alpha}$ and $\bar{C}_l = \hat{C}_l/C_{N\alpha}$ remained unchanged after convergence. However, the estimation values of coefficients $\hat{C}_{m\alpha}$ and \hat{C}_l were varied with $C_{N\alpha}$; thus, a correct value of $C_{N\alpha}$ must be given in advance to identify the aerodynamic coefficients themselves using the present model. In order to make a direct comparison with the results of the K-model, the values of $C_{N\alpha}$ were all taken to be correct in the previous computations, and thus the coefficients themselves can be easily obtained from the coefficient ratios. It was interesting that the K-model yielded relatively accurate co-

Table 3 Capabilities of estimating the coefficients and their ratios for both models

The value ^a of $C_{N\alpha}$ in filter	K-model $\hat{C}_{m\alpha}$	Present model $\hat{C}_{m\alpha}$	K-model $\hat{C}_{m\alpha}$	Present model $\hat{C}_{m\alpha}$ ^b
4.0	-0.6981	-0.6990	-0.1745	-0.1748
4.4	-0.6983	-0.7689	-0.1587	-0.1748
6.4	-0.6993	-1.1180	-0.1093	-0.1747

^a $C_{N\alpha}$ is 4.0 rad⁻¹ for generating measurements. ^bTrue value of $\hat{C}_{m\alpha}$ is -0.1750.

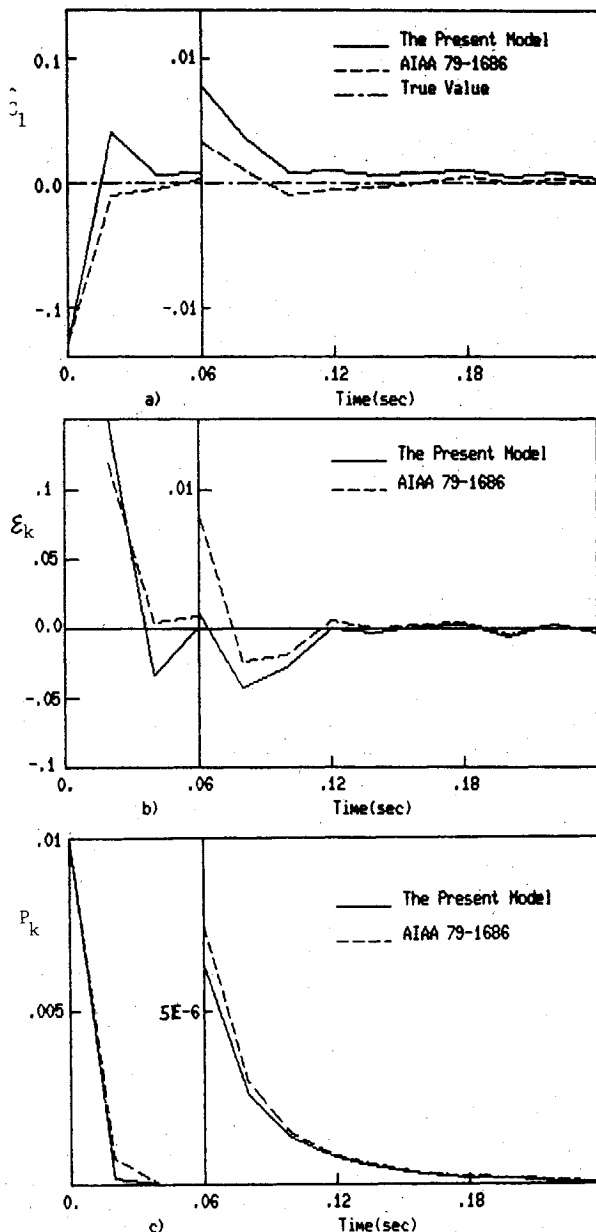


Fig. 5 Rolling moment coefficient: a) estimate; b) gain innovations product; c) variance.

efficients $\hat{C}_{m\alpha}$ and \hat{C}_b , which were not sensitive to variations of the value of $C_{N\alpha}$, as we found in the computations. For instance, if the values of $C_{N\alpha}$ were increased up to 4.4 and 6.4 before filtering with the K-model, the resulting values of $\hat{C}_{m\alpha}$ and \hat{C}_b were varied slightly after convergence. This is probably because higher flight altitudes resulted in lower dynamic pressure, and so the aerodynamic normal force had little effects on the vehicle motions. Therefore, the correct value of $C_{N\alpha}$ must be given in advance to identify the aerodynamic

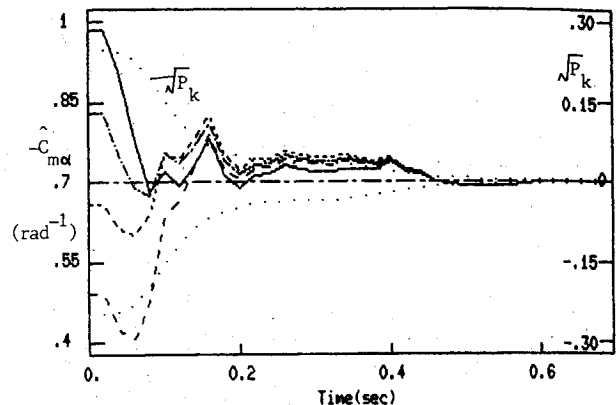


Fig. 6 Four filtering histories in different initial conditions.

coefficient ratios using the K-model. Table 3 illustrates the presented circumstances.

The primary reasons for choosing $C_{N\alpha}$ as a denominator of the coefficient ratios in the present model are as follows: 1) the $C_{N\alpha}$ is not easy to correctly identify with respect to other parameters if it is augmented into the parameter vector, particularly at higher altitudes; 2) from the viewpoint of aerodynamics, at a small angle of attack, normal force derivative $C_{N\alpha}$ is a comparatively stable parameter that is not sensitive to the slight changes of vehicle shape and to variations of flow states.

The results of the K-model listed in Table 2 are not very consistent with the corresponding results of Kelsey's original paper.³ For T_f and $\hat{C}_{m\alpha}$, the results of the present paper are better. This is because in improving the computation speed, Ref. 3 did not pursue a high accuracy of numerical integration, which was taken to be consistent with the errors of noise disturbances. But in the present paper, a fourth-order Runge-Kutta scheme was uniformly used, leading to higher accuracy. The computation time T_c of the present paper was about six times that of Ref. 3 because the CDC 6600 computer was used in Ref. 3 as opposed to the slower 320-type computer used here. In addition, the higher computation accuracies in this paper also increased the values of T_c . However, all of these differences have no effect on the verification of the contents of this paper. In the computations, both models were treated in the same manner, and, thus, the relative quantities between them can sufficiently explain problems.

Finally, note that both the present model and the K-model assumed that the measurements of u , v , and w were available. This assumption is still not very practical in some cases. Based upon the present model, another model has been developed using $h = [a_x a_y a_z p q r]^T$ instead of $h = [u v w p q r]^T$ and including nonlinear and bias moment terms in the vector C . The model has successfully been applied to a postflight aerodynamic identification of one re-entry satellite.

Conclusions

Given the discussed conditions, through analyses, numerical simulations, and comparisons, the major conclusions are

as follows:

1) The six-degree-of-freedom model presented in this paper can accurately estimate aerodynamic coefficient ratios or derivative ratios, including the important static stability margin, without the somewhat impractical assumptions about altitude measurements and atmospheric modeling made in Kelsey's model.

2) Kelsey's model and the present model possess equivalent real-time estimation capability and accuracy.

3) The errors caused by the model simplifications have little effect on the estimation results.

References

¹Siemers, P. M. and Larson, T. J., "Space Shuttle Orbiter and Aerodynamic Testing," *Journal of Spacecraft and Rockets*, Vol. 16, July/Aug. 1979, pp. 223-231.

²Ohodsimski, D. E., Golubef, U. F., and Siharlulidse, U. G., "Algorithms for Control of Spacecraft Entering into Atmosphere," *Science*, Moscow, 1975, pp. 271-304.

³Kelsey, J. R., "Real-Time Estimation of Aerodynamic Coefficients by Means of an Extended Kalman Filter," Sandia Laboratories, Albuquerque, NM, SAND78-2032, Feb. 1979.

⁴Kelsey, J. R. and Petersen, D. P., "Aerodynamic Coefficient Estimation By Means of An Extended Kalman Filter," AIAA Paper 79-1686, Aug. 1979.

⁵Quanwei, J., Jinzhi, X., and Shuying, Z., "Determination of Aerodynamic Coefficients for a Re-entry Body by Means of an Extended Kalman Filter," *Acta Aeronautica et Astronautica Sinica*, Vol. 3, Sept. 1982, pp. 15-24.

⁶Quanwei, J., Jiongang, C., and Shuying, Z., "A Parametric Study for Identification of Aerodynamic Coefficients of Re-entry Body Using Kalman Filter," *Journal of Chinese Society of Astronautics*, Oct. 1983, pp. 13-22.

*Recommended Reading from the AIAA
Progress in Astronautics and Aeronautics Series . . .*



Thermal Design of Aeroassisted Orbital Transfer Vehicles

H. F. Nelson, editor

Underscoring the importance of sound thermophysical knowledge in spacecraft design, this volume emphasizes effective use of numerical analysis and presents recent advances and current thinking about the design of aeroassisted orbital transfer vehicles (AOTVs). Its 22 chapters cover flow field analysis, trajectories (including impact of atmospheric uncertainties and viscous interaction effects), thermal protection, and surface effects such as temperature-dependent reaction rate expressions for oxygen recombination; surface-slip equations for low-Reynolds-number multicomponent air flow, rate chemistry in flight regimes, and noncatalytic surfaces for metallic heat shields.

TO ORDER: Write AIAA Order Department,
370 L'Enfant Promenade, S.W., Washington, DC 20024

Please include postage and handling fee of \$4.50 with all orders.
California and D.C. residents must add 6% sales tax. All orders under
\$50.00 must be prepaid. All foreign orders must be prepaid. Please allow
4-6 weeks for delivery. Prices are subject to change without notice.

1985 566 pp., illus. Hardback

ISBN 0-915928-94-9

AIAA Members \$49.95

Nonmembers \$74.95

Order Number V-96